Bioresource Technology 361 (2022) 127714

Contents lists available at ScienceDirect

Bioresource Technology

journal homepage: www.elsevier.com/locate/biortech

Revealing the key role of structural cross-link between lignin and polysaccharides during fast pyrolysis of lignocellulose

Yingchuan Zhang [a,b], Weiting Xu [c], Nianfang Ma [a], Yu Shen [d], Feixiang Xu [e], Yitong Wang [f], Nannan Wu [g], Zhengxiao Guo [b], Liqun Jiang [a,e,*]

[a] Guangdong Engineering Laboratory of Biomass High-value Utilization, Guangdong Plant Fiber Comprehensive Utilization Engineering Technology Research and Development Center, Guangzhou Key Laboratory of Biomass Comprehensive Utilization, Institute of Biological and Medical Engineering, Guangdong Academy of Sciences, Guangzhou 510316, China
[b] Department of Chemistry, The University of Hong Kong, Hong Kong, China
[c] College of Chemical Engineering, Beijing University of Chemical Technology, Beijing 10029, China
[d] State Key Laboratory of Microbial Technology, Institute of Microbial Technology, Shandong University, Qingdao 266237, China
[e] Guangzhou Institute of Energy Conversion, Chinese Academy of Sciences, Guangzhou 510640, China
[f] College of Metallurgy and Energy, North China University of Science and Technology, 21 Bohai Street, Tangshan 063210, China
[g] Department of Green Chemistry and Technology, Ghent University, Ghent 9000, Belgium

HIGHLIGHTS

- Cross-linked lignin was estimated with carboxymethylation-separation analytic method.
- Pyrolytic behavior of cross-linked lignin was significantly distinguished from free lignin.
- Cross-linked lignin was 7.2 times efficient in promoting small molecule generation.
- Cross-linked lignin was 2.7 times efficient in promoting aromatic generation.
- Ring scission and dehydration rearrangement were enhanced by cross-linked lignin.

GRAPHICAL ABSTRACT

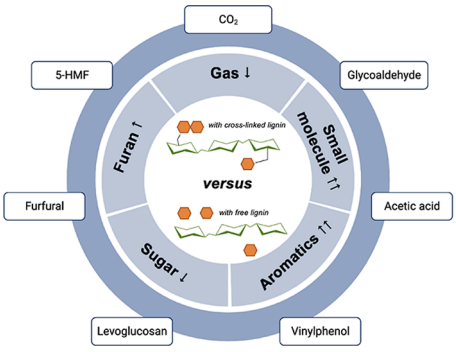

ARTICLE INFO

Keywords:
Lignocellulose valorization
Structural cross-link
Lignin-carbohydrate complex
Fast pyrolysis

ABSTRACT

Lignin-carbohydrate complex (LCC) is the native existing form of major components in lignocellulose. In this study, the structural cross-link between lignin and polysaccharides in lignocellulose was quantitatively estimated with carboxymethylation-separation (CM-Sep) method, and its influence on lignocellulose pyrolysis was systematically investigated. The cross-linked lignin was found to positively correlate with the production of small molecules and furan derivatives while negatively affecting the generation of anhydrous sugars. Content of small molecules was increased by 97% while that of anhydrous sugars was decreased by 47% in pyrolytic products with levoglucosan yield lowered by 54 wt% in the existence of cross-linked lignin. Furthermore, the impact of

* Corresponding author at: Guangdong Engineering Laboratory of Biomass High-value Utilization, Guangdong Plant Fiber Comprehensive Utilization Engineering Technology Research and Development Center, Guangzhou Key Laboratory of Biomass Comprehensive Utilization, Institute of Biological and Medical Engineering, Guangdong Academy of Sciences, Guangzhou 510316, China.
E-mail address: lqjiang@ms.giec.ac.cn (L. Jiang).

https://doi.org/10.1016/j.biortech.2022.127714
Received 21 June 2022; Received in revised form 26 July 2022; Accepted 27 July 2022
Available online 30 July 2022

cross-linked lignin was revealed to be significantly distinguished from free lignin. Impeded glycosidic end formation and boosted glycosyl ring scission as well as lignin fragmentation were responsible for the distinction. Excellent correlations between structural cross-link and lignocellulose pyrolytome could facilitate product prediction and process design.

1. Introduction

Lignocellulose is an abundant natural resource with promising potential to supply the renewable energy sector's growing needs. In general, lignocellulose is comprised of cellulose, hemicellulose and lignin components, which can be further valorized to versatile commercial products via separation and conversion (Clomburg et al., 2017). However, native lignin and cellulose are largely connected by covalent linkages (aromatic α-O-4 and β-O-4 ether bonds), resulting in lignin-carbohydrate complex (LCC) forming. A network of hydrogen bonds also exists between lignin and polysaccharides. These interactions feature a highly random cross-linked structure between the components, and render the plant cell wall excellent integrity and rigidity (Afzal et al., 2022). There are a large volume of published studies describing the recalcitrant LCC structure in biorefinery (Zhao et al., 2020). One solution is selective saccharification of LCC by economic and efficient fast pyrolysis (Wang et al., 2022).

Fast pyrolysis is a thermo-chemical technology that is typically performed in the absence of oxygen at 450–600 °C in very short residence time. Levoglucosan is the major product from pyrolytic saccharification of lignocellulose, with a maximal yield of 70.1 wt% (Lin and Lu, 2021). The feasibility of levoglucosan used as substrate for downstream bioprocess has been well demonstrated before (Jiang et al., 2019). Thus far, fast pyrolysis to saccharify lignocellulose has been particularly highlighted in biorefinery. Firstly, this process requires seconds or minutes rather than hours or even days. Then, fast pyrolysis can be performed without any catalysts such as corrosive acids or expensive enzymes. Furthermore, highly concentrated levoglucosan has been delicately obtained via pyrolytic process, leading to low-cost purification. Most importantly, pyrolytic saccharification of lignocellulose shows economic benefits over the traditional hydrolysis conversion (Bhar et al., 2022). Therefore, fast pyrolysis is being updated with technology development toward efficient lignocellulose utilization.

Previous studies have reported complicated interactions among three major components during lignocellulose pyrolysis. The native stoichiometry of lignin and polysaccharides in lignocellulose was found to significantly affect the pyrolytic behavior (Hosoya et al., 2007). Interactions between lignin-cellulose and lignin-hemicellulose have been further reported with a huge impact on pyrolytic product distribution (Wang et al., 2011). This work further compared co-pyrolysis of lignin-hemicellulose and cellulose-hemicellulose, indicating that production of 2-furfural and acetic acid from hemicellulose was slightly enhanced in the existence of cellulose while significantly inhibited with addition of isolated lignin. Cellulose-lignin co-pyrolysis at different temperatures further demonstrated the role of lignin in promoting the production of small molecules (*e.g.* esters, aldehydes, and ketones) and inhibiting the formation of anhydrous sugars (mainly levoglucosan) (Wu et al., 2016). Besides, natural cellulose-hemicellulose and cellulose-lignin binary models were generated to compare their pyrolytic behaviors, and product analysis suggested that the cellulose-lignin interaction was much more impactful than cellulose-hemicellulose interaction (Zhang et al., 2015). This work also revealed that native lignin in lignocellulose could remarkably diminish the production of levoglucosan and promote the formation of low-weight molecules (*e.g.* ethylene) and gas (*e.g.* CO_2).

Although these studies have reported the general effects of lignin on lignocellulose pyrolysis, there is no comprehensive inspection on the cross-linked structure between lignin and polysaccharides because of lacking quantitative tools (Long and Antoniewicz, 2014; Zhou et al., 2010). Since lignin would be covalently conjunct or labile in lignocellulose, it is of great significance to distinguish and estimate these existing forms especially after amelioration pretreatment for achieving favorable valorization processes. Herein, the pyrolytic behavior of structural cross-link between lignin and polysaccharides was comprehensively studied by precisely modulating lignin and hemicellulose removal in natural lignocellulose. In order to estimate cross-linked lignin, a novel carboxymethylation-separation (CM-Sep) method was designed. Covalent bonds between lignin and polysaccharides were quantified by counting phase-separated fractions. Elemental, composition analysis, and Fourier transform infrared (FTIR) spectroscopy further proved the accuracy of CM-Sep method. At last, fast pyrolysis of tailored lignocellulose was monitored with GC–MS, and effects of cross-linked structure on content and yields of pyrolysis products were systematically investigated. Insightful mapping of product distribution and mechanism behind it were provided by introducing new parameters and correlations that were associated with structural cross-link in lignocellulose.

2. Materials and methods

2.1. Preparation of lignocellulose samples

Before use, reed rods were pulverized to 60–80 mesh and then dried at 105 °C until constant weight. Reed rods were first Soxhlet-extracted with ethanol–benzene (1:2, v/v) at 80 °C for 4 h to remove plant fats and waxes. Lignin in extracted biomass was removed by following the $NaClO_2$-oxidation (Ox) delignification process (Wang et al., 2021). For one repeat, in brief, biomass (2 g) was suspended in 300 mL water and then $NaClO_2$ (0.8 g) and acetic acid (160 μL) were sequentially added. The mixture was stirred at 70 °C for 1 h, and the residual was collected by vacuum filtration and washed with deionized water thoroughly. This process was conducted on extracted biomass for 0, 1, 2, 3, 5 repeats to give Ox-0-Ox-5 samples. Hemicellulose-free biomass was obtained by following a standard hydrothermal (HTL) process performed at 180 °C for 12 h (Kim and Lee, 2006). Oxidation process was also proceeded on hemicellulose-free biomass for 0, 1, 2 repeats to give HTL-Ox-0-HTL-Ox-2 samples. At the last step, all samples were stirred in 0.5 wt% H_2SO_4 solutions (20 mL) at room temperature for 1 h to remove metals, and the solid was collected by filtration, washed by deionized water thoroughly, and freeze dried before characterization and fast pyrolysis.

2.2. Isolation of lignin

To test the effect of free lignin on fast pyrolysis, featured lignin from Ox and HTL-Ox groups was isolated according to previous method (Bauer et al., 2012). In brief, 5 g raw reed rod was suspended in a 100 mL mixture of ethanol-HCl (95:5, v/v). The mixture was stirred under reflux at 80 °C for 8 h, and then filtered and washed with ethanol to collect the filtrate. The solution was concentrated to 100 mL by vacuum evaporation, and then resuspended in 400 mL cold HCl solution (1:600, v/v) for recrystallization overnight. The solid was collected by centrifugation, filtered, washed by deionized water thoroughly and then freeze dried.

2.3. Characterization of lignocellulose

Elemental analyzer (Vario EL cube, Elementar, Germany) was used to determine the content of organic elements (C, H, N) in biomass samples. The content of alkali and alkaline earth metals (AAEMs) was detected by an inductively coupled plasma emission spectrometer (ICP-

Table 1
Componential and elemental analysis of lignocellulose.

Samples	Component				Organic element			AAEMs			
	Cellulose (wt%)	Hemicellulose (wt%)	Lignin (wt%)	C/L	C (wt%)	H (wt%)	C/H	Na (ppm)	K (ppm)	Mg (ppm)	Ca (ppm)
Raw	53.1	18.9	23.5	2.3	46.4	5.9	7.9	543.2	3396.2	231.2	1055.8
Ox-0	45.6	24.9	19.6	2.3	46.9	6.1	7.8	115.8	38.0	12.7	124.7
Ox-1	48.7	25.6	14.2	3.4	44.7	6.1	7.3	148.7	42.7	10.7	91.6
Ox-2	50.1	25.5	12.1	4.1	44.0	6.0	7.3	129.2	44.0	10.2	123.8
Ox-3	53.1	25.9	8.0	6.6	43.0	6.0	7.2	154.9	47.2	10.4	91.6
Ox-5	56.5	26.3	6.9	8.2	42.5	6.1	7.0	133.1	47.1	12.7	119
HTL-Ox-0	44.1	0.0	54.9	0.8	52.5	5.9	8.9	125.5	37.8	13.7	93.4
HTL-Ox-1	52.8	0.0	40.7	1.3	50.3	5.9	8.5	146.1	42.0	15.1	121.3
HTL-Ox-2	78.4	0.0	24.6	3.2	46.6	6.0	7.7	156.3	52.1	15.6	109.8

OES, OPTIMA 8000DV, PerkinElmer, United States). Composition of cellulose, hemicellulose and lignin in biomass was quantified according to the protocol issued by National Renewable Energy Laboratory (NREL) (Sluiter et al., 2004). Scanning electron microscope (SEM) morphology was recorded on a cold field emission scanning electron microscope (S-4800, Hitachi, Japan). FTIR was recorded on an infrared spectrometer (TENSOR27, Bruker, Germany).

2.4. CM-Sep estimation of cross-linked lignin in lignocellulose

Lignocellulose samples were carboxymethylated to facilitate the estimation of cross-linked lignin and ^{1}H NMR test. In brief, 1 g sample was suspended in 50 mL of isopropanol with vigorous stirring at room temperature, and then 5 mL of 7.5 M NaOH solution was dropwise added carefully. After 1 h stirring, 1.5 g monochloroacetic acid was added, and the mixture was heated to 55 °C and stirred for another 3 h. After neutralizing the mixture with acetic acid, the solid was collected by filtration and resuspended in 200 mL of 80% methanol solution. The solid was collected by filtration and washed with absolute methanol (20 mL) twice to remove water. It was finally dried in a vacuum oven at 40 °C for 12 h to give the carboxymethylated samples. For quantitative estimation of cross-linked lignin, carboxymethylated sample was suspended in 100 mL water and the mixture was stirred at room temperature for 1 h. The insoluble and soluble fractions were separated by centrifugation and filtration, and washed with excess water and acetone sequentially. Water-insoluble fraction was directly freeze dried, while water-soluble fraction was first condensed by vacuum evaporation and then freeze dried. Polysaccharide composition in soluble and insoluble fractions was quantified by ^{1}H NMR (Bruker 600 M, Germany). To prepare NMR samples, the solid was hydrolyzed in 2 mL of 25% D_2SO_4 in D_2O at 90 °C for 2 h, and then the filtrated solution was introduced into NMR tube. The peak assignment on ^{1}H NMR spectra was concluded (see Supplementary material). Relative content of glucose, mannose, xylose was determined according to the integrals, as well as degree of substitution (DS) calculated by formula (1).

$$DS_{NMR} = \frac{\text{sum of integral of methylene protons at C2, C3, and C6}}{\text{integral of anomeric protons}} \quad (1)$$

2.5. Fast pyrolysis

Fast pyrolysis was performed on a semi-batch CDS reactor (Pyroprobe 5200, CDS Analytical, United States) in duplicate. The reaction temperature was 500 °C and heating rate was 20 K·ms^{-1}. High-purity helium was set at 20 mL/min to sweep the resulting volatiles through a 300 °C transmission line into the gas chromatography-mass spectrometry (GC–MS) system (GC-7890A, MS-5975C, Agilent Technologies, United States) for separation and detection. Specifically, pyrolysis volatiles were separated by DB-1701 capillary column. GC oven temperature was maintained at 40 °C for 3 min, then increased from 40 °C to 280 °C at a rate of 5 °C/min, and finally maintained at 280 °C for 8 min. Mass spectrometer parameters included ion source temperature of 230 °C, quadrupole temperature of 150 °C, ion source energy of 70 eV, and a scan range (m/z) of 29 to 450 amu. Relative content of compounds and levoglucosan yield were calculated according to formulas (2) and (3), respectively.

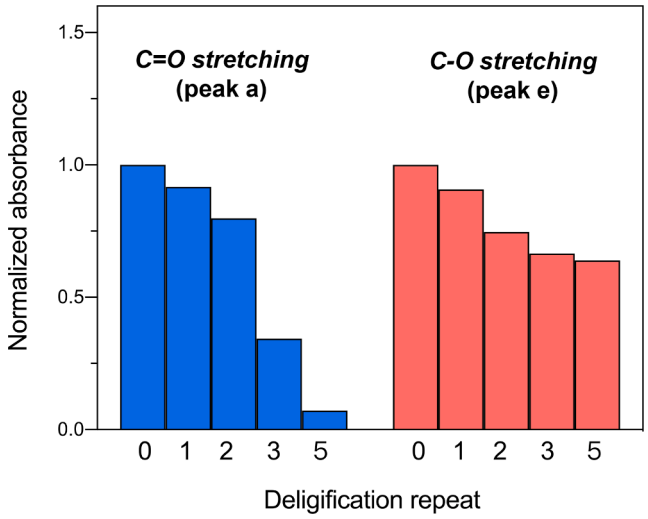

Fig. 1. Normalized characteristic peak intensity of peak a and e in different Ox samples.

$$\text{Relative content}\,(\%) = \frac{\text{area of specific compound}}{\text{total area of all compounds}} \times 100\% \quad (2)$$

$$\text{Levoglucosan yield}\,(wt\%) = \frac{\text{levoglucosan mass}}{\text{biomass mass} \times \text{cellulose content}} \times 100\% \quad (3)$$

3. Result and discussion

3.1. Characterization of lignocellulose samples

The content of major elements and components in raw and treated lignocellulose samples was shown in Table 1. For each repeat, around 3% lignin was removed in Ox group, while delignification was more efficient in HTL-Ox group as up to 15%. The difference could be explained by the capacity of hemicellulose in stabilizing the whole networks and maintaining branches during delignification and solvent elution. The increased cellulose-to-lignin (C/L) ratio also validated the efficiency of the delignification process. Besides, the diminished carbon-to-hydrogen (C/H) elemental ratio further demonstrated the removal of lignin, because the C/H ratio of lignin (11.1) was much higher than that of cellulose (7.5) and hemicellulose (7.2) (Zhang et al., 2022). Notably, the catalytic effect of metals in all samples has been excluded by removing AAEMs with diluted acid to obtain negligible concentrations.

To *in site* confirm the difference in cross-link structure derived from

Table 2
Mass distribution of carboxymethylated fractions after phase separation.

Samples	Insoluble fraction (wt%)	Soluble fraction (wt %)	IS/S Ratio	DS	Cross-linked lignin (wt%)
Ox-0	54.1	45.9	1.18	1.73	17.9
Ox-1	49.4	50.6	0.98	1.41	9.2
Ox-2	47.6	52.4	0.91	1.50	7.9
Ox-3	43.4	56.6	0.77	1.35	3.9
Ox-5	40.2	59.8	0.67	1.77	1.9
HTL-Ox-0	51.0	49.0	1.04	0.85	18.8
HTL-Ox-1	44.0	56.0	0.79	0.73	2.4
HTL-Ox-2	41.7	58.3	0.71	0.74	0.3

delignification, the morphology of Ox-0 and Ox-5 was observed by SEM (see Supplementary material). Compared to Ox-0, the surface of delignified Ox-5 was irregularly coarse, with random distribution of pores. These pores were the sites where cross-linked lignin located before delignification (Yang et al., 2020; Yu et al., 2022). Meanwhile, the remaining lignin particles in Ox-5, which tended to aggregate due to hydrogen and hydrophobic bonding, were much smaller and relatively separated as compared to Ox-0. FTIR spectrum of Ox samples further demonstrated the gradient removal of cross-linked lignin (see Supplementary material). Characteristic peaks of lignin included C═O stretching for peaks a and b (1593–1609 cm^{-1} and 1505–1511 cm^{-1}), C—H deformation for peaks c and d (1462 cm^{-1} and 1425 cm^{-1}), C—O stretching for peak e (1268 cm^{-1}), and C—H out-of-plane stretching for peak f (840 cm^{-1}). The intensities of these peaks were gradually weakened or even vanished from Ox-0 to Ox-5. further depicted the normalized intensities of C—O bonding peaks was further depicted in Fig. 1. Notably, close-to-zero intensity was observed for C═O stretching peak on behalf of lignin carbonyls, while only a slight decrease was observed for C—O stretching in Ox-5. Since C—O stretching mainly occurred in α-O-4 and β-O-4 ether bonds responsible for lignin-lignin and lignin-polysaccharide connections, the difference between C—O and C═O stretching intensity demonstrated that cross-linked lignin was retained while labile lignin was removed. Taken together, these results suggested that lignocellulose samples with different level of cross-linked lignin, have been successfully constructed by repeated $NaClO_2$-Ox process.

3.2. CM-Sep estimation of cross-linked lignin

Carboxymethylcellulose is a traditional functional polymer obtained by chemical modification on natural cellulose. In this process, side-chain hydroxyl groups were substituted by hydrophilic carboxymethyl groups, thus facilitating water absorbency of the resulting polymer. The water-soluble capacity could be reflected by estimating DS, and carboxymethylcellulose with DS > 0.6 was soluble in pure water (Barbucci et al., 2000). However, hydrophobic cross-linkers on side chains have been validated to decrease the hydrophilicity of polymers. For example, hydrogels with a high density of cross-linkers would lose their solubility and swelling capacity in aqueous condition, because the rigid cross-linked structure was much difficult to expand (Barbucci et al., 2000). Inspired by the aromatic nature of lignin, an analytic strategy based on carboxymethylation modification, has been developed for the estimation of cross-linked lignin in lignocellulose.

After carboxymethylation, lignocellulose sample was separated into water-soluble and water-insoluble fractions, according to their cross-linked lignin content. As shown in Table 2, both the mass ratio of insoluble fraction-to-soluble fraction (IS/S ratio) and detectable lignin content decreased from Ox-1 to Ox-5. There was only few lignin detected in soluble fractions, which was corresponded with the aforementioned side-chain effect and previous results (Jin et al., 2010). Only insoluble fraction was considered to cross-link with lignin. Therefore, the IS/S ratio might be highlighted as a potential important factor to quantitatively estimate the cross-linked lignin in lignocellulose. To prove its feasibility, the correlation between IS/S ratio and original lignin content calculated by NREL method, and correlation between IS/S ratio and elemental C/H ratio, were described in Fig. 2. Excellent coefficients in Ox group was observed (R^2 = 0.998 and 0.914, respectively), and the slight deviation in HTL-Ox group could be explained by an additional carbonization effect to generate partially fragmented side-chain lignin in severe conditions of HTL process. Meanwhile, the IS/S ratio was found to correlate better with lignin content than C/H ratio. In sum, the IS/S ratio has been proved as a robust factor for quantitative estimation of cross-linked lignin in lignocellulose.

Carboxymethylated samples could be further subjected to ^{1}H NMR test to detect polysaccharide composition. To date, ^{1}H NMR was rarely used in component quantification in lignocellulose, since sugar-ring anomeric protons have split chemical shifts in high field and their conformation would be interconverted depending on temperature (Duus et al., 2000). So far, most polysaccharide composition was quantified with 2D Correlation Spectroscopy (COSY NMR) in a tedious process. However, after carboxymethylation, active hydroxyls (with quick deuterium exchange effect before) were converted to carboxymethyls with stable methylene protons. Their signals could be collected and discriminated with fixed NMR chemical shift after degradation of polysaccharides. In general, the signal of α-anomeric glycosyl was found in the low field (5.20–5.50 ppm) as compared to β-anomeric protons (4.60–4.80 ppm), and protons of glucose appeared lowly as compared to xylose and mannose. Details of chemical shifts for carboxymethylated polysaccharide monomers were concluded (see Supplementary material). Carboxymethylated polysaccharide composition in insoluble fractions was further calculated from integrals as reported before (Petzold et al., 2006). Notably, negligible mannose, arabinose, and galactose were found in insoluble fractions, while the glucose content was much higher than original content in lignocellulose calculated by NREL

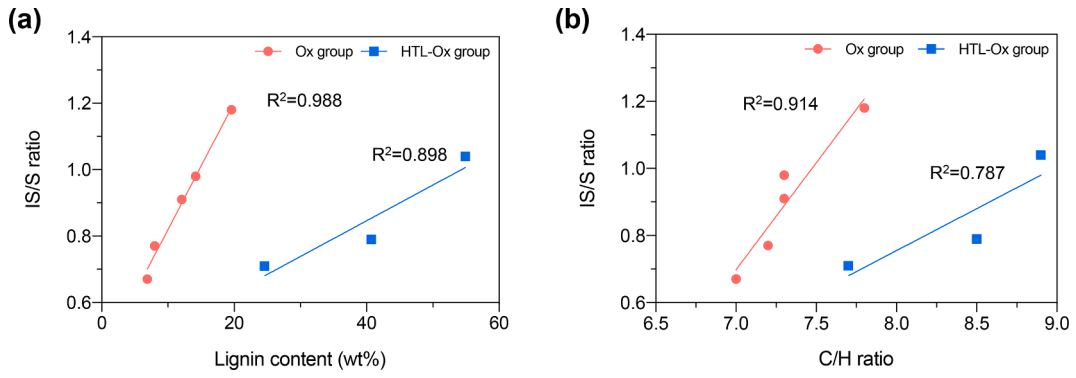

Fig. 2. Linear correlations between IS/S ratio and (a) lignin content and (b) elemental C/H ratio.

Table 3
Distribution of major pyrolytic products in natural biomass group.

Category	Compound name	Relative content (%)								
		Raw	Ox-0	Ox-1	Ox-2	Ox-3	Ox-5	HTL-Ox-0	HTL-Ox-1	HTL-Ox-2
Gas	Carbon dioxide	9.7	5.9	6.1	6.8	7.1	11.7	6.6	9.2	9.7
C1-C3	Formaldehyde	0.0	1.6	0.0	0.0	0.1	0.1	0.0	0.0	0.0
Small	Acetaldehyde	0.6	0.4	0.4	0.1	0.0	0.1	0.1	0.0	0.1
Molecules	Glycolaldehyde	1.8	1.4	1.1	1.0	0.6	0.6	0.3	0.5	1.1
	Acetic acid	3.8	3.4	2.8	3.0	1.9	1.5	0.5	0.4	0.4
	Methyl glyoxal	1.8	1.2	1.1	1.0	0.8	0.9	0.5	0.6	0.8
	Hydroxypropanone	0.0	0.4	0.4	0.4	0.2	0.2	0.2	0.2	0.4
	Pronanal	0.1	0.4	0.1	0.2	0.1	0.1	0.3	0.1	0.0
	Methyl formate	0.3	0.2	0.1	0.1	0.1	0.1	0.5	0.1	0.1
C4-C5	5-HMF	0.5	2.2	2.2	0.9	1.8	1.0	0.6	0.8	1.4
Furans	Furfural	1.4	1.6	2.2	1.3	1.7	1.3	0.8	0.7	0.9
	Furan	0.2	0.2	0.3	0.6	0.4	0.5	0.3	0.2	0.2
	2,5-Dimethyl furan	0.4	0.1	0.2	0.1	0.2	0.2	0.2	0.1	0.2
	2-Methoxy furan	0.0	0.1	0.1	0.1	0.1	0.1	0.0	0.2	0.0
	2-Methyl furan	0.0	0.2	0.4	0.4	0.5	0.5	0.4	0.2	0.2
	2-Furanone	0.0	0.5	0.4	0.3	0.3	0.3	0.1	0.2	0.2
Sugars	Levoglucosan	14.2	24.7	38.2	45.1	46.0	46.1	44.3	49.3	53.1
	Levoglucosenone	0.0	0.1	0.1	0.2	0.3	0.5	0.8	0.3	0.3
	1,4:3,6-Dianhydro-α-D-glucopyranose	0.4	0.2	0.7	0.5	0.6	1.0	1.1	0.7	0.8
Aromatics	2-Methoxy-4-vinylphenol	0.3	0.8	0.5	0.3	0.3	0.3	0.0	0.0	0.0
	3,5-Dimethoxy-4-hydroxytoluene	0.0	1.9	1	1.7	1.7	1.5	0.8	0.2	0.2
	Other phenyl compounds	4.3	4.4	3.0	2.1	1.8	1.5	5.8	4.1	2.3

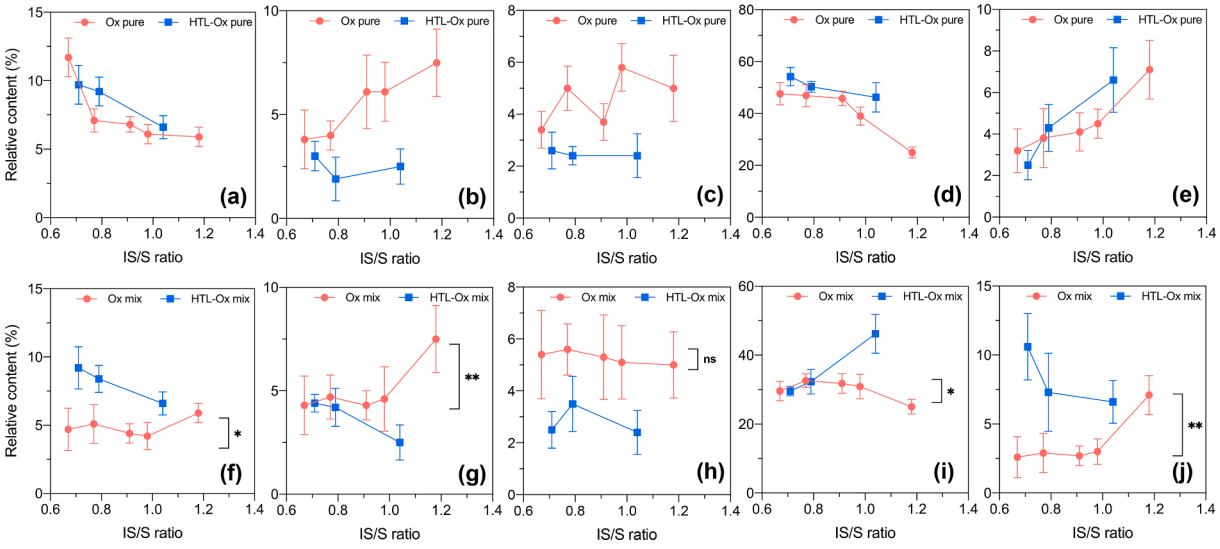

Fig. 3. Correlations between relative content of (a, f) gas, (b, g) C1-C3 small-molecule compounds, (c, h) C4-C6 furan derivatives, (d, i) C5-C6 anhydrous sugars, and (e, j) aromatic compounds and IS/S ratio (P-value: ** < 0.01, * < 0.05; ns: not significant).

method. This could be explained the fact that cellulose was more accessible to cross-link with lignin than hemicellulose (Jin et al., 2010). Expectedly, there was no hemicellulose component detected in HTL-Ox group. In carboxymethylated glucose, the signals of methylene protons (glycolic O-CH2-) found in 4.20–4.55 ppm, which were sharp and intense peaks, were assigned to carboxymethyl groups at C3, C2α, C2β, and C6 from the low to high field, respectively. By comparing the integrals of methylene protons with anomeric protons, DS in carboxymethylated samples was calculated by following formula (1). As shown in Table 2, in general, DS in all samples was higher than 0.6, which suggested the original solubility of polysaccharide chains in lignocellulose samples. However, due to the existence of cross-linked lignin networks, they have completely lost the water solubility and consequently been precipitated during phase-separation process. Furthermore, DS on different positions in each sample was calculated respectively (see Supplementary material), and the relative reactivity of hydroxyl groups was found as –OH(6) > –OH(2) > –OH(3) during carboxymethylation. This order was identical with previous results, and had been explained by the difference in formation of hydrogen bonding, which could hierarchically hinder the substitution reaction during carboxymethylation (Sabari et al., 2017).

3.3. *Evaluating the effect of cross-linked lignin on lignocellulose pyrolysis*

The product distribution for pyrolysis of lignocellulose samples was shown in Table 3. Products were first divided into five groups, including gas (CO_2), C1-C3 small-molecule compounds (*e.g.* glycolaldehyde, methyl glyoxal and acetol), C4-C6 furan derivatives (*e.g.* 2(5H)-furanone, 2-furaldehyde and 5-HMF), C5-C6 anhydrous sugars (*e.g.* levoglucosan), and aromatics. For each category, integrated content was correlated with IS/S ratio to quantitatively evaluate the effect of cross-linked lignin. As shown in Fig. 3a-e, except for the case of C4-C6 furan derivates, there were regular positive or negative correlations in both Ox and HTL-Ox samples, which demonstrated that the cross-linked lignin

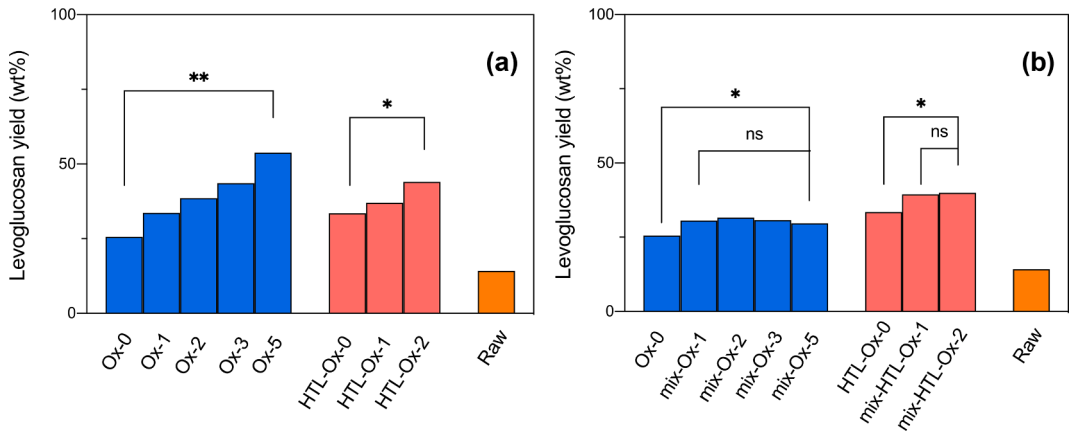

Fig. 4. Levoglucosan yield of different samples of (a) natural complex group and (b) physical mixture group.

level was highly associated with lignocellulose pyrolysis. The fluctuating correlation for furan products was probably due to the relative high existence of hemicellulose in Ox samples. As is reported, hemicellulose could significantly contribute to the production of C4-C6 furan derivates as compared to cellulose in lignocellulose pyrolysis (Qaseem et al., 2021). Neglectable and irregular levels of hemicellulose in Ox samples shown in Table 1, could also support this reason. The regular correlations between IS/S ratio and product content were in accordance with previous results, where the increased lignin level would result in the decreased content of C5-C6 anhydrous sugars (47.6% in Ox-5 *vs* 25.0% in Ox-0), meanwhile increasing the content of aromatic lignin derivatives (3.2% in Ox-5 *vs* 7.1% in Ox-0) (Zhang et al., 2015). Levoglucosan yield also demonstrated the role of lignin, as the value was increased from 26.0 wt% to 53.8 wt% after 5 repeats in Ox-5 and from 33.5 wt% to 44.1 wt% after 3 repeats in HTL-Ox-2 (Fig. 4a).

Interestingly, CO_2 production was significantly enhanced by 2.3 times after 5 repeated

removal of lignin. This enhancement was contrary to previous study (Zhang et al., 2015). Although CO_2 could be generated from polysaccharides and lignin during fast pyrolysis, it has been reported that lignin would release more CO_2 than cellulose (Yang et al., 2015). In this study, however, Ox-5 with lowest lignin level was found to generate more CO_2 than others. This could be explained by the huge difference between product content of anhydrous sugars content (25% in Ox-0 *vs* 47% in Ox-5) and that of aromatics (7% in Ox-0 *vs* 3% in Ox-5), which was associated with less efficient CO2 release during lignin fragmentation than cellulose degradation. In FTIR analysis, unremoved lignin in Ox-5 has been proven to cross-link with polysaccharides, thus further limiting its fragmentation to generate CO_2. The IS/S ratio of Ox-5 (0.67) further validated the existence of cross-linked lignin, which highlighted the importance of discriminating cross-linked lignin from free lignin to evaluate their pyrolytic behaviors respectively.

By comparing Ox with HTL-Ox samples, hemicellulose was found to impact the pyrolytic behavior even under similar levels of cross-linked lignin. Although the regular of product distribution in HTL-Ox group was accordant with that in Ox group, more efficient decrease in small molecule production (Fig. 3b) and increase in gas and sugar formation (Fig. 3a and d) were observed after comparing HTL-Ox to Ox samples with similar IS/S ratio. There was only slight difference in gas formation. Notably, a similar fluctuation between IS/S ratio and content of furan derivatives was not observed among HTL-Ox samples, which was associated with the regular gradient of lignin level in HTL-Ox group. Taken together, with reference to IS/S ratio, the role of cross-linked lignin during fast pyrolysis of lignocellulose was revealed. One was further impacted by the existence of hemicellulose, especially for the production of small-molecule and sugar products.

Table 4
Distribution of major pyrolytic products in physical mixture group.

Category	Compound name	Relative content (%)						
		Raw	mix-Ox-1	mix-Ox-2	mix-Ox-3	mix-Ox-5	mix-HTL-Ox-1	mix-HTL-Ox-2
Gas	Carbon dioxide	9.7	4.2	4.4	5.1	4.7	8.4	9.2
C1-C3	Formaldehyde	0.0	0.1	0.0	0.1	0.1	0.0	0.0
Small	Acetaldehyde	0.6	0.0	0.0	0.0	0.0	0.0	0.0
Molecules	Glycolaldehyde	1.8	0.1	0.2	0.3	0.3	1.6	1.9
	Acetic acid	3.8	2.6	2.0	2.5	1.9	0.7	0.7
	Methyl glyoxal	1.8	0.9	1.3	1.1	1.8	1.1	1.2
	Hydroxypropanone	0.0	0.4	0.5	0.2	0.8	0.4	0.5
	Pronanal	0.1	0.1	0.2	0.3	0.5	0.3	0.1
	Methyl formate	0.3	0.1	0.2	0.2	0.3	0.1	0.1
C4-C5	5-HMF	0.5	2.0	2.2	2.1	2.0	1.6	1.6
Furans	Furfural	1.4	2.4	2.4	2.8	2.4	0.8	0.5
	Furan	0.2	0.2	0.3	0.2	0.2	0.3	0.0
	2,5-Dimethyl furan	0.4	0.1	0.2	0.2	0.1	0.2	0.0
	2-Methoxy furan	0.0	0.0	0.0	0.0	0.1	0.0	0.0
	2-Methyl furan	0.0	0.2	0.3	0.0	0.3	0.4	0.1
	Furanone	0.0	0.2	0.3	0.3	0.3	0.2	0.3
Sugars	Levoglucosan	14.2	30.0	31.1	32.0	29.1	31.9	29.1
	Levoglucosenone	0.0	0.4	0.3	0.2	0.2	0.0	0.2
	1,4:3,6-Dianhydro-α-D-glucopyranose	0.4	0.5	0.4	0.4	0.3	0.4	0.3
Aromatics	2-Methoxy-4-vinylphenol	0.3	1.1	0.8	0.9	1.0	1.1	2.4
	3,5-Dimethoxy-4-hydroxytoluene	0.0	0.4	0.3	0.4	0.3	1.2	1.1
	Other phenyl compounds	4.3	1.5	1.6	1.6	1.3	5.0	7.1

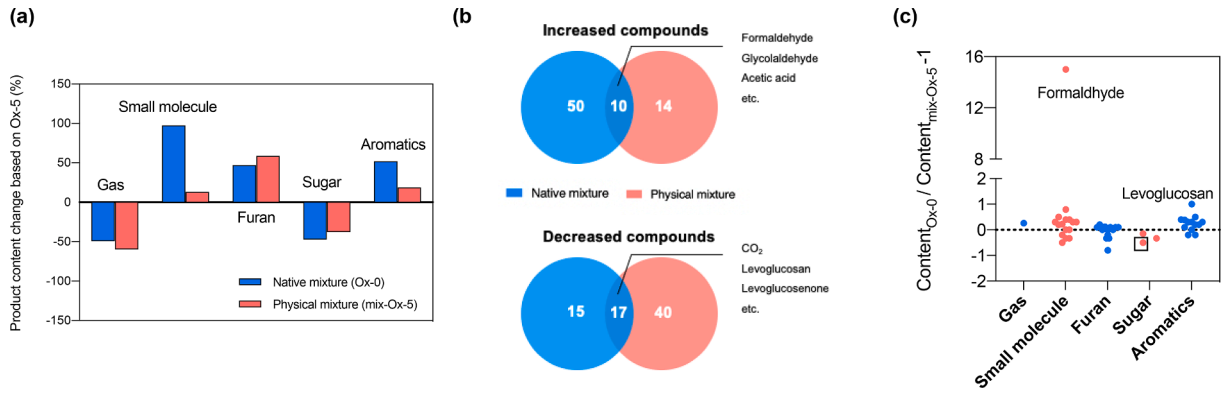

Fig. 5. (a) Product content change of major compounds in native mixture (Ox-0) and physical mixture (mix-Ox-5) compared to Ox-5; (b) number of compounds with increased or decreased content in two mixtures compared to Ox-5; (c) product content change by comparing native mixture with physical mixture.

3.4. Comparing the effect of cross-linked lignin and free lignin on lignocellulose pyrolysis

To compare the effect of cross-linked lignin with that of free lignin during pyrolysis, isolated lignin was externally added to Ox samples (namely mix-Ox samples), and HTL-Ox samples (namely mix-HTL-Ox samples). Ideally, mix-Ox-1-mix-Ox-5 and mix-HTL-Ox-1-mix-HTL-Ox-2 were modulated with overall lignin level that was the same as Ox-0 and HTL-Ox-0, respectively. These physical mixtures were then subjected to pyrolysis-GS-MS, and product distribution was shown in Table 4. Product content of physical mixture (with free lignin) was then compared with the corresponding native samples Ox-0 or HTL-Ox-0 (with cross-linked lignin) in Fig. 3f-j. Under the same level of lignin, compared to native Ox-0, physical mixture mix-Ox-5 exhibited a 3.3% decrease in content of C1-C3 small molecules compounds ($P < 0.01$). This was mainly attributed to 1.5% and 1.3% decrease in generation of formaldehyde and glycolaldehyde, respectively. CO_2 production was sightly decreased from 5.9% to 4.7%. Offset was the production of C5-C6 anhydrous sugars, which was significantly enhanced from 25% to 32% content in Fig. 3i as well as a 16% increase in levoglucosan yield in Fig. 4b ($P < 0.05$). Notably, after a comparison among physical mixtures, it could be found that only a slight variation was observed in both product content and levoglucosan yield. Thus, it should be noted that the pyrolytic behavior of cross-linked lignin was markedly different from that of free lignin.

In this study, by highlighting IS/S ratio facilitated by CM-Sep method, content of cross-linked lignin was correlated with pyrolytic production. Effect of free lignin and cross-linked lignin on pyrolytic product distribution was further discriminated and systematically evaluated. The content change of major categories in Ox-0 and mix-Ox-5 in comparison with lignin-free Ox-5 was depicted in Fig. 5a to evaluate the impact of two lignin-addition methods. In general, both ways could boost the production of C1-C3 small molecules and C4-C5 furan derivatives. However, cross-linked lignin was found to promote the generation of small molecules more efficiently (differ by 7.5 times), while free lignin enhanced the production of furans. Since C1-C3 small molecules were the next-step products of furans from cellulose degradation, the offsetting effect was observed between cross-linked lignin and free lignin (Paine et al., 2008). Similarly, offsetting changes were observed in gas and C5-C6 anhydrous sugar production that was much less obvious than generation of small molecules and furans. Notably, cross-linked lignin was much more productive (2.7 times) in promoting aromatics formation as compared to free lignin, with an increase of 52% in Ox-0 *versus* 18% in mix-Ox-5. This demonstrated that cross-linked lignin was easier to be fragmented than free lignin in fast pyrolysis.

An elaborate mapping of all detected pyrolytic products (namely

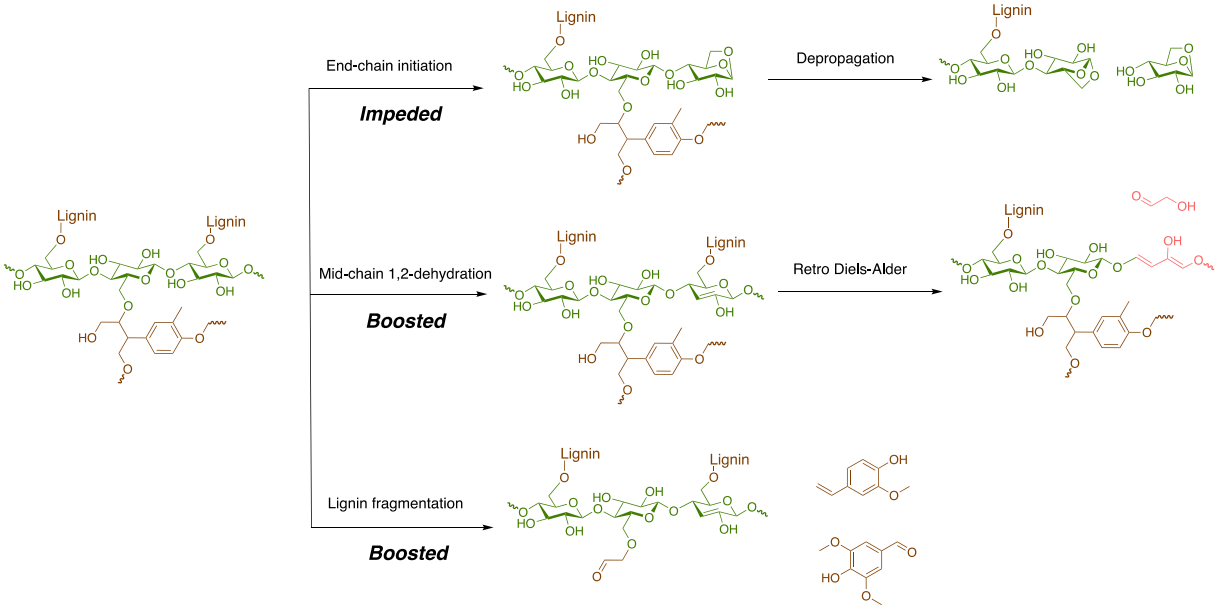

Fig. 6. Illustration of effect of cross-linked lignin on reaction pathways in fast pyrolysis of lignocellulose.

pyrolytome analysis) in native and physical mixture was compared in Fig. 5b. In general, 60 out of 92 pyrolytic products were increased after addition of cross-linked lignin *versus* 24 of 81 products in free lignin-added sample. 10 small-molecule compounds such as formaldehyde, glycolaldehyde, and acetic acid were highlighted in the overlap area. For the lowering group, 17 compounds were found in the overlap area, especially CO_2, levoglucosan, and levoglucosenone as excellent feedstocks in biorefinery. Notably, Ox process significantly reduced the content and species of fermentative-toxic furans and phenols during pyrolysis as compared to HTL treatment, which could be utilized to endorse the downstream enzymatic hydrolysis. Content change of all detected products in overlap area of Ox-0 and mix-Ox-5 was further mapped in Fig. 5c. These points were observed to aggregate together, with only formaldehyde and levoglucosan rarely outstanding. This further demonstrated the potential use of IS/S ratio in predicting product distribution in the future.

3.5. Mechanism of cross-linked lignin in lignocellulose pyrolysis

Effect of cross-linked lignin was explained in terms of two processes—cellulose degradation and lignin fragmentation. Fast pyrolysis facilitated stagewise thermal degradation of cellulose. It has been well accepted that there were two competitive reaction pathways (intermolecular C—C bond cleavage *versus* intramolecular glycosidic bond cleavage) at the first degradation stage, leading to different fates of glycan units (Patwardhan et al., 2009). Vinu et al. demonstrated a continuous concerted chain-reaction with the move-up of levoglucosy end-groups, resulting in glycosidic bond cleavage and levoglucose release (Vinu and Broadbelt, 2012). In contrast, a set of complex reaction pathways concerning sugar-ring C—C bond cleavage would generate small-molecule and furan products instead of levoglucosan (Paine et al., 2007). In this work, given the diminished anhydrous sugar content and increased content of C—C bond cleavage products in native mixture, the cross-linked lignin was proven to enhance the second set of reaction pathways competing with glycosidic bond cleavage. This was consistent with previous studies on biomass co-pyrolysis, where this effect was explained by glycosyl C_6 existence of side-chain lignin (Zhang et al., 2015). Interestingly, in physical mixture, there was only a slight increase in levoglucosan yield with a decreased IS/S ratio under the same lignin level, meaning that this change could not be predicated with reference to an overall lignin level applied in most previous research. The boosted production of levoglucosan associated with decreased cross-link was much less evident than directly removing lignin component. As illustrated in Fig. 6, the covalent bonds between lignin and the polysaccharide C_6-oxygen, which were responsible for the structural cross-link in lignocellulose, would result in less efficient release of levoglucosyl end-groups. By dominating the C_6-oxygen, they could prevent the anhydro-ring closure that was necessary for levoglucosan formation. As a result, competitive reactions such as ring scission and dehydration rearrangement were conversely promoted, leading to C1-C3 small molecule formation (Patwardhan et al., 2009). Besides, the enhancement on C—C bond cleavage by cross-linked lignin was not found in hemicellulose-free groups. Instead, in native mixture the levoglucosan production was enhanced while the small molecule production was diminished. This difference could be contributed to the maintenance role of hemicellulose. Removal of hemicellulose would lead to an incomplete biomass cross-linked structure, thus facilitating the thermal energy access to internal cellulose chain instead of lignin network and consequently promoting glycosidic bond cleavage. The effect of collapsing cross-linked structure had also been demonstrated in a study regarding thermal pretreatment of lignocellulose (Zhang et al., 2022). Compared to corresponding native mixtures, lignin content in mix-Ox-5 was diminished *versus* an increased lignin content in hemicellulose-removed mix-HTL-Ox-2. It further demonstrated the crucial role of hemicellulose for maintaining cross-linked biomass structure and influencing pyrolytic pathways, and also highlighted the usefulness of the IS/S ratio factor.

According to the results, except for inhibiting glycosidic bond cleavage while enhancing glycosyl ring scission, glycosyl C_6 existence of lignin could also promote the fragmentation of connected lignin polymer. Despite β-O-4 ether bonds with relatively high bond association energy (52–72 kcal mol^{-1}), transformation of function groups in lignin aromatic rings was capable to activate the lignin depolymerization under mild conditions (Wu et al., 2018). This effect was probably similar to the case of lignocellulose with side-chain linked to polysaccharides. Besides, favorable reaction kinetics of lignin under fast heating rates—with an activation energy E_a of 120–143 kJ/mol—supported the boosted generation of aromatics from cross-linked lignin (Chen et al., 2020). In short, both the activation effect of side-chain and favorable kinetics were responsible for lignin fragmentation, demonstrating the crucial role of cross-linked lignin during fast pyrolysis of lignocellulose.

4. Conclusion

This study comprehensively illustrated the unique role of structural cross-link by inspecting the lignin-polysaccharides interactions in terms of product distribution and yields during fast pyrolysis of lignocellulose. Cross-linked lignin in LCC was quantitatively estimated by CM-Sep method. The presence of cross-linked lignin was revealed to significantly enhance the production of small molecules and furan derivatives meanwhile hindering the generation of anhydrous sugars by up to 47%. Furthermore, compared to free lignin, cross-linked lignin was found to impact lignocellulose pyrolysis more robustly by enhancing glycosyl ring scission and lignin fragmentation.

CRediT authorship contribution statement

Yingchuan Zhang: Data curation, Methodology, Formal analysis, Investigation, Writing – original draft. **Weiting Xu:** Data curation, Writing – review & editing. **Nianfang Ma:** Data curation, Formal analysis. **Yu Shen:** Data curation, Writing – review & editing. **Feixiang Xu:** Data curation, Formal analysis. **Yitong Wang:** Data curation, Formal analysis. **Nannan Wu:** Data curation, Formal analysis. **Zhengxiao Guo:** Supervision, Writing – review & editing. **Liqun Jiang:** Conceptualization, Supervision, Funding acquisition, Writing – review & editing.

Declaration of Competing Interest

The authors declare that they have no known competing financial interests or personal relationships that could have appeared to influence the work reported in this paper.

Data availability

Data will be made available on request.

Acknowledgement

This work was funded by GDAS' Project of Science and Technology Development (No. 2022GDASZH-2022010110), Guangdong Basic and Applied Basic Research Foundation (No. 2021A1515012063), the Foundation of State Key Laboratory of Utilization of Woody Oil Resource (No. GZKF202116), Innovation Research Group Project of Natural Science Foundation of Hebei Province (No. E2022209093), and the Special Support Program of Guangdong Province (2019TQ05N232).

Appendix A. Supplementary data

Supplementary data to this article can be found online at https://doi.org/10.1016/j.biortech.2022.127714.

References

Afzal, R.A., Pennells, J., Yamauchi, Y., Annamalai, P.K., Nanjundan, A.K., Martin, D.J., 2022. Lignocellulosic plant cell wall variation influences the structure and properties of hard carbon derived from sorghum biomass. Carbon Trends 7, 100168. https://doi.org/10.1016/j.cartre.2022.100168.

Barbucci, R., Magnani, A., Consumi, M., 2000. Swelling behavior of carboxymethylcellulose hydrogels in relation to cross-linking, pH, and charge density. Macromolecules 33, 7475–7480. https://doi.org/10.1021/ma0007029.

Bauer, S., Sorek, H., Mitchell, V.D., Ibáñez, A.B., Wemmer, D.E., 2012. Characterization of Miscanthus giganteus lignin isolated by ethanol organosolv process under reflux condition. J. Agric. Food Chem. 60, 8203–8212. https://doi.org/10.1021/jf302409d.

Bhar, R., Tiwari, B.R., Sarmah, A.K., Brar, S.K., Dubey, B.K., 2022. A comparative life cycle assessment of different pyrolysis-pretreatment pathways of wood biomass for levoglucosan production. Bioresour. Technol. 356, 127305 https://doi.org/10.1016/j. biortech.2022.127305.

Chen, W.H., Eng, C.F., Lin, Y.Y., Bach, Q.V., 2020. Independent parallel pyrolysis kinetics of cellulose, hemicelluloses and lignin at various heating rates analyzed by evolutionary computation. Energy Convers. Manage. 221, 113165 https://doi.org/10.1016/j.enconman.2020.113165.

Clomburg, J.M., Crumbley, A.M., Gonzalez, R., 2017. Industrial biomanufacturing: The future of chemical production. Science 80, 355. https://doi.org/10.1126/science.aag0804.

Duus, J., Gotfredsen, C.H., Bock, K., 2000. Carbohydrate structural determination by NMR spectroscopy: modern methods and limitations. Chem. Rev. 100, 4589–4614. https://doi.org/10.1021/cr990302n.

Hosoya, T., Kawamoto, H., Saka, S., 2007. Cellulose-hemicellulose and cellulose-lignin interactions in wood pyrolysis at gasification temperature. J. Anal. Appl. Pyrol. 80, 118–125. https://doi.org/10.1016/j.jaap.2007.01.006.

Jiang, L.Q., Fang, Z., Zhao, Z.L., Zheng, A.Q., Wang, X.B., Li, H.B., 2019. Levoglucosan and its hydrolysates via fast pyrolysis of lignocellulose for microbial biofuels: A state-of-the-art review. Renew. Sustain. Energy Rev. 105, 215–229. https://doi.org/10.1016/j.rser. 2019.01.055.

Jin, Z.F., Yu, Y.M., Shao, S.L., Ye, J.W., Lin, L., Iiyama, K., 2010. Lignin as a cross-linker of acrylic acid-grafted carboxymethyl lignocellulose. J. Wood Sci. 56, 470–476. https://doi.org/10.1007/s10086-010-1128-z.

Kim, T.H., Lee, Y.Y., 2006. Fractionation of corn stover by hot-water and aqueous ammonia treatment. Bioresour. Technol. 97, 224–232. https://doi.org/10.1016/j.biortech.2005.02. 040.

Lin, E.Y., Lu, C., 2021. Development perspectives of promising lignocellulose feedstocks for production of advanced generation biofuels: A review. Renew. Sustain. Energy Rev. 136, 110445 https://doi.org/10.1016/j.rser.2020.110445.

Long, C.P., Antoniewicz, M.R., 2014. Quantifying biomass composition by gas chromatography/mass spectrometry. Anal. Chem. 86, 9423–9427. https://doi.org/10.1021/ac502734e.

Paine, J.B., Pithawalla, Y.B., Naworal, J.D., Thomas, C.E., 2007. Carbohydrate pyrolysis mechanisms from isotopic labeling. Part 1: The pyrolysis of glycerin: Discovery of competing fragmentation mechanisms affording acetaldehyde and formaldehyde and the implications for carbohydrate pyrolysis. J. Anal. Appl. Pyrol. 80 (2), 297–311.

Paine, J.B., Pithawalla, Y.B., Naworal, J.D., 2008. Carbohydrate pyrolysis mechanisms from isotopic labeling. Part 2. The pyrolysis of D-glucose: General disconnective analysis and the formation of C-1 and C-2 carbonyl compounds by electrocyclic fragmentation mechanisms. J. Anal. Appl. Pyrol. 82, 10–41. https://doi.org/10.1016/j.jaap.2008.01.002.

Patwardhan, P.R., Satrio, J.A., Brown, R.C., Shanks, B.H., 2009. Product distribution from fast pyrolysis of glucose-based carbohydrates. J. Anal. Appl. Pyrol. 86, 323–330. https://doi.org/10.1016/j.jaap.2009.08.007.

Petzold, K., Schwikal, K., Heinze, T., 2006. Carboxymethyl xylan-synthesis and detailed structure characterization. Carbohydr. Polym. 64, 292–298. https://doi.org/10.1016/j. carbpol.2005.11.037.

Qaseem, M.F., Shaheen, H., Wu, A.M., 2021. Cell wall hemicellulose for sustainable industrial utilization. Renew. Sustain. Energy Rev. 144, 110996 https://doi.org/10.1016/j.rser.2021.110996.

Sluiter, A., Hames, B., Ruiz, R.O., Scarlata, C., Sluiter, J., Templeton, D., 2004. Determination of structural carbohydrates and lignin in biomass. Biomass Anal. Technol. Team Lab. Anal. Proced. 1–14.

Vinu, R., Broadbelt, L.J., 2012. A mechanistic model of fast pyrolysis of glucose-based carbohydrates to predict bio-oil composition. Energy Environ. Sci. 5, 9808–9826. https://doi.org/10.1039/c2ee22784c.

Wang, S., Guo, X., Wang, K., Luo, Z., 2011. Influence of the interaction of components on the pyrolysis behavior of biomass. J. Anal. Appl. Pyrol. 91, 183–189. https://doi.org/10.1016/j.jaap.2011.02.006.

Wang, Y., Yang, Y., Qu, Y., Zhang, J., 2021. Selective removal of lignin with sodium chlorite to improve the quality and antioxidant activity of xylo-oligosaccharides from lignocellulosic biomass. Bioresour. Technol. 337 https://doi.org/10.1016/j.biortech. 2021.125506.

Wang, J., Zhang, B., Aldeen, A.S., Mwenya, S., Cheng, H., Xu, Z., Zhang, H., 2022. Enhancing production of hydrocarbon-rich bio-oil from biomass via catalytic fast pyrolysis coupled with advanced oxidation process pretreatment. Bioresour. Technol. 359, 127450 https://doi.org/10.1016/j.biortech.2022.127450.

Wu, X., Fan, X., Xie, S., Lin, J., Cheng, J., Zhang, Q., Chen, L., Wang, Y., 2018. Solar energy-driven lignin-first approach to full utilization of lignocellulosic biomass under mild conditions. Nat. Catal. 1, 772–780. https://doi.org/10.1038/s41929-018-0148-8.

Wu, S., Shen, D., Hu, J., Zhang, H., Xiao, R., 2016. Cellulose-lignin interactions during fast pyrolysis with different temperatures and mixing methods. Biomass Bioenergy 90, 209–217. https://doi.org/10.1016/j.biombioe.2016.04.012.

Yang, H.M., Appari, S., Kudo, S., Hayashi, J.I., Norinaga, K., 2015. Detailed chemical kinetic modeling of vapor-phase reactions of volatiles derived from fast pyrolysis of lignin. Ind. Eng. Chem. Res. 54, 6855–6864. https://doi.org/10.1021/acs.iecr.5b01289.

Yang, X., Zheng, A., Zhao, Z., Xia, S., Wang, Q., Wei, G., Huang, Z., Jiang, L., Wang, S., Li, H., 2020. Maximizing production of sugar and ultrafine lignin particles from recalcitrant softwood by different acids-assisted organosolvolysis and fast pyrolysis. J. Clean. Prod. 276, 122827 https://doi.org/10.1016/j.jclepro.2020.122827.

Yu, S., Yang, X., Zhao, P., Li, Q., Zhou, H., Zhang, Y., 2022. From biomass to hydrochar: Evolution on elemental composition, morphology, and chemical structure. J. Energy Inst. 101, 194–200. https://doi.org/10.1016/j.joei.2022.01.013.

Zhang, J., Choi, Y.S., Yoo, C.G., Kim, T.H., Brown, R.C., Shanks, B.H., 2015. Cellulose-hemicellulose and cellulose-lignin interactions during fast pyrolysis. ACS Sustain. Chem. Eng. 3, 293–301. https://doi.org/10.1021/sc500664h.

Zhang, Y., Xu, F., Chen, F., Zhang, Y., Wu, Y., Jiang, L., 2022. Dual utilization of lignocellulose biomass and glycerol waste to produce fermentable levoglucosan via fast pyrolysis. Front. Chem. 10, 1–8. https://doi.org/10.3389/fchem.2022.847767.

Zhao, Y., Shakeel, U., Saif Ur Rehman, M., Li, H., Xu, X., Xu, J., 2020. Lignin-carbohydrate complexes (LCCs) and its role in biorefinery. J. Clean. Prod. 253, 120076.

Zhou, Y., Stuart-Williams, H., Farquhar, G.D., Hocart, C.H., 2010. The use of natural abundance stable isotopic ratios to indicate the presence of oxygen-containing chemical linkages between cellulose and lignin in plant cell walls. Phytochemistry 71, 982–993. https://doi.org/10.1016/j.phytochem.2010.03.001.